*J. Min. Metall. Sect. B-Metall. 58 (1) (2022) 43 - 49*

**Journal of Mining and Metallurgy, Section B: Metallurgy**

# PRIMARY MICROSTRUCTURE CHARACTERIZATION OF Co-20Ni-9Al-7W-3Re-2Ti SUPERALLOY

**A. Tomaszewska**

The Silesian University of Technology, Department of Materials Technologies, Katowice, Krasinski, Poland
The Silesian University of Technology, The Silesian Laboratory of Aviation Technologies, Katowice, Krasinski, Poland

*(Received 09 March 2021; accepted 03 September 2021)*

***Abstract***

*The characterization of the primary microstructure of the new Co-based superalloy of Co-20Ni-9Al-7W-3Re-2Ti type was shown in this article. The investigated alloy was manufactured by induction melting process from pure feedstock materials. The fundamental technological problem related to Co-Al-W-X multicomponent alloys casting process is a strong susceptibility to interdendritic segregation of alloying elements, especially tungsten and rhenium. The performed analysis revealed that the observed effect of alloying elements segregation was detectable and much stronger than for Co-9Al-9W and Co-20Ni-7Al-7W alloys, related to titanium, nickel, and aluminium migration to inter-dendritic spaces. Consequently, the tungsten concentration gradient between dendritic and interdendritic zones was higher than for Co-9Al-9W and Co-20Ni-7Al-7W alloys. The same situation was in the case of rhenium and cobalt, but Co concentration in the interdendritic zone was only slightly lower.*

***Keywords:*** *Co-Al-W alloys; New Co-based superalloys; Primary microstructure; Interdendritic segregation*

## 1. Introduction

Superalloys based on Ni or Co are high-performance materials usually used in high-temperature elements of land-based and aircraft turbines such as discs, blades, rotating shafts, nozzle guide vanes, and combustor liners [1]. Between them, the Co-based superalloys have applications as critical turbine engine parts, where hot corrosion, wear, and oxidation resistance is required [2-4]. Due to relatively low mechanical properties, especially at high temperature, the conventional Co-based superalloys are not dedicated to high-performance structural elements of turbines such as blades and disk. However, they can be used for static-loaded parts, e.g., vanes. The lower applications possibilities of carbides strengthened Co-based superalloys is related to temperature-depended limitation of strengthening effect by carbides precipitation in Co-based matrix [2]. The most popular and widely used alloys from this group are Haynes 188, Mar-M and stellite. Those alloys are strengthened by solid solution Coss and carbides of refractory elements. Still, its high-temperature properties, such as creep resistance, are lower than Ni-based superalloys due to lack of γ/γ′ structure [5-7].

Recent investigations showed that there is the possibility of beneficial γ/γ′ structure creation in Co-based superalloys. In the Co-Al system, the phase $Co_3Al$ (similar to $Ni_3Al$ phase in Ni-based systems) generally does not exist, and precipitation of an equilibrium B2-CoAl phase is more likely [8, 9]. However, the $Co_3Al$ phase with $L1_2$ type of lattice was detected occasionally in some of the grains of Co-Al ferromagnetic shape memory alloys [10]. Simultaneously in the Co-X (X=W, Nb, Ta) systems, compounds $Co_3X$ with ordered $L1_2$ structure (γ′) has been reported [11-14], but these phases are not stable at the higher temperature (> 600 °C) [10, 15-17]. The $Co_3X$ $L1_2$ ordered phases are characterized by cuboidal shape, similar to $Ni_3(Al, Ti)$ phase in the Ni-based superalloys [18] and transform at the higher temperature to equilibrium disordered form with the same formula $Co_3X$ but with topological close-packed morphology $D0_{19}$ type of lattice [19-21]. The metastability of $Co_3X$ phases with refractory elements can be weakened by forming triple phases such as $Co_3(Al, X)$. The presence of this type of compound was detected in the analysis of alloys that formed the Co-Al-W system. The additive and the appropriate proportion of Al and W in the structure, thereby stabilized the $L1_2$ ordered structure of $Co_3(Al, W)$

*Corresponding author: agnieszka.tomaszewska@polsl.pl

***https://doi.org/10.2298/JMMB210309044T***

phase up to 900 °C [15,16]. Mo's addition should get similar structural effects with additional decreasing of alloys density as an alloying element. However, the maximal level of Mo replacement was only up to 3 at %, because with the higher content of this alloying element, the formation of equilibrium $Co_3Mo$ phase with ordered $D0_{19}$ structure was expected. This type of precipitates was characterized by specific needle-like morphology favoring the cracking phenomena with a strongly brittle character [22].

Compared to $Co_3$(Al, W), no data confirmed $Co_3$(Al, Mo) phase with $L1_2$ type of structure. $L1_2$ ordering does not take place on ageing between 600 °C and 800 °C [16]. This transformation was detected in the cases of quaternary alloys of Co-Al-Mo-Nb/Ta type. It was revealed that Nb or Ta's small addition played a critical role in stabilizing of γ-γ′ microstructure [18, 22, and 23]. First principle calculations of $Co_3$(Al, Mo, Nb) phase with the $L1_2$ structure revealed that this phase was mechanically stable and possessed intrinsic ductility. It was additionally found that the shear and Young's moduli of $Co_3$(Al, Mo, Nb) were smaller than those of $Co_3$(Al, W) [24].

Based on those considerations, the new group of materials based on Co-Al-X systems (where X were refractory elements such as W – tungsten-containing alloys, and Mo, Nb or Ta – tungsten-free alloys) were developed [15, 16, 18, 22, 23]. The main strengthening element in those alloys was the ordered $L1_2$ phase with the overall formula $Co_3$(Al, X). This new class of γ′ precipitates strengthened Co-based materials revealed higher solidus and liquidus temperatures and less segregation during solidification than traditional Ni-based superalloys [25]. The γ′ precipitates and the low-energy γ/γ′ interface provided high-temperature strength and stability to these alloys similar to the Ni-based superalloys. Intensive investigations in alloying strategy (increasing γ′ solvus temperature and growing strength and yield stress) got beneficial effects. At this moment, the creep properties and flow stress of tertiary, quaternary and quinary new Co-based superalloys are comparable to Ni-based superalloys of the first and second generation at a temperature approaching 900 °C [15, 25]. But there are still challenges that require further research: decreasing the density of alloys and improving their creep and oxidation resistance [26, 27].

In the case of increasing of γ′ solvus temperature and increasing strength and yield stress, only data for Co-Al-W are present in the literature. It can be assumed that to increase the γ′ solvus temperature and improve the microstructural stability, alloying elements, such as Ti, V, Ta, Nb, Mo, and Ni, should be added. Such elements increase the γ′ solvus temperature in the following order: Ta←Nb←Ti←V←Mo←Ni [28, 29]. The latest conclusion presented in [29] revealed that Nb greatly destabilized the γ′ phase and was not suggested for alloy design in the Co-9Al-9W system. The morphologies and volume fractions of phases observed in these alloys' microstructures were highly sensitive to alloying with elements like Ni, Ti, Mo, B, Cr, and Ta [28, 30-33]. Co-based alloys' creep resistance is increased mainly with the addition of Cr, Mo, Ti, and Ta [34-36], and oxidation resistance could be improved primarily by expansion of Cr, Si, and Ta [37-39]. The reduction of alloys density partially replaced W by Mo, Nb, and Ta or developing tungsten free alloys.

The aim of the research is to characterize the primary microstructure of a new cobalt-based alloy with the addition of Re and Ti in as cast condition. The role of rhenium was to increase the melting point of the alloy, while titanium should increase the temperature of the $L1_2$ solvus. It was assumed that the dominant part of rhenium would be located in the cobalt solid solution, while titanium would form the $L1_2$ phase.

## 2. Materials and methods

The nominal composition of the new cobalt-based superalloy Co-20Ni-9Al-7W-3Re-2Ti used in this investigation was shown in Table 1. The induction vacuum process was used for alloy preparation. The process was made in a VSG 02 Balzers type furnace, and the alloy was manufactured in $Al_2O_3$ crucible. The manually compacted molding sand Konmix MAPI was used to set the alumina crucible in the furnace coil. Argon of ALPHAGAZTM 1Ar (99,999% Ar) type was used for protection of liquid metal. Before the process started, an operating chamber was washed by argon blowing (3 times). After this, the working pressure was decreased to a value of 10^-3Tr (~0.13 Pa). The furnace chamber pressure was increased to 600 Tr (8×10^4 Pa) by Ar filling in the next step. Technically pure metals were utilized as a stock material: electrolytic Co and Ni (both min. 99.98%), Al (purity 99.98%) and W, Re, and Ti. Alloying Co, Ni, and Al elements were added to the crucible in the first step before the melting process. The other alloying elements – W, Re, and Ti- were added to Co-Ni-Al's liquid solution after its high-temperature homogenization (ca. 1600 °C). The final liquid alloy was thermally treated in a temperature range of 1650÷1750 °C for 10 minutes. The final alloy was

***Table 1.*** *Nominal composition of investigated alloy*

| Alloy | Co | Ni | Al | W | Re | Ti |
|---|---|---|---|---|---|---|
| At. % | Bal. | 20 | 9 | 7 | 3 | 2 |
| Wt % | Bal. | 17.2 | 3.56 | 18.86 | 8.18 | 2.1 |

cast to the rods form under a protective argon atmosphere into cold graphite molds (Fig. 1). The actual composition of final alloy was shown in Table 2.

***Figure 1.*** *General view of final-cast from Co-20Ni-9Al-7W-3Re-2Ti alloy*

The scanning electron microscopy (SEM-Hitachi S-3400N) was used for the characterization of microstructural elements of alloys, as well as the chemical composition in micro-areas (EDS - Thermo NORAN System Seven), and phase identification (EBSD - INCA HKL Nordlys II, Channel 5).

To ensure excitation of spectral lines of all analyzed elements during the EDS analysis, the primary electron beam variable energy was used. Phase identification was performed by the EBSD method and was based on comparing the experimental Kikuchi pattern with the theoretical pattern. The “macro” phase constituent analysis of the investigated alloy was developed by X-ray diffraction method using X`Pert 3 diffractometer. The light microscopic analysis of microstructure was performed by Nikon Eclipse MA200 microscopy. The final sample was cut from the central part of the rod, then a metallographic sample was prepared, and the plates were ground, polished, and etched. The electrolytic etching in a solution containing 25 ml $H_2O$, 50 ml HCl, 15 g $FeCl_3$, and 3 g $CuCl_2 \times NH_4Cl \times 2H_2O$ was used to microstructure disclosure.

## 3. Results and discussion

The phase composition analysis of Co-20Ni-9Al-7W-3Re-2Ti alloy in the as-cast state (obtained by XRD measurement) showed diffraction peaks corresponding only to Co solid solution lattice - ICDD pattern no 15-0806 (Fig. 2). No peaks ordered for expected compounds of Co-W, Co-Ti or other types were identified.

The primary microstructure (Fig. 3), visible in the longitudinal cross-section, consisted of a very thin, peripheral chill zone (not shown in Figure 3), and a wide columnar grain zone stretching to the core of the primary cast rod. The direction of columnar crystals growth was following the direction of heat dissipation from solidifying ingot. The rode center was occupied by a thick zone of refined, equiaxed grains, crystallized ahead of the columnar front.

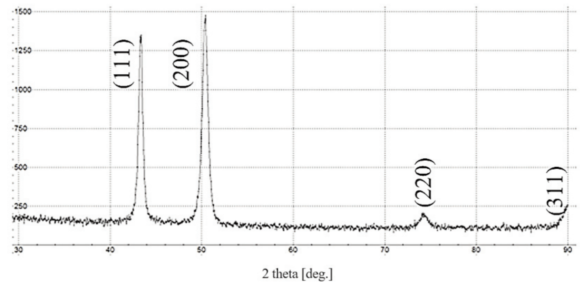


***Figure 2.*** *Phase constituent of Co-20Ni-9Al-7W-3Re-2Ti alloy – XRD analysis*

***Table 2.*** *Actual composition of investigated alloy*

| Alloy | Co | Ni | Al | W | Re | Ti |
|---|---|---|---|---|---|---|
| At. % | Bal. | 19.58 | 8.75 | 7.11 | 2.87 | 2.1 |
| Wt % | Bal. | 15.99 | 3.01 | 19.35 | 7.58 | 2.15 |

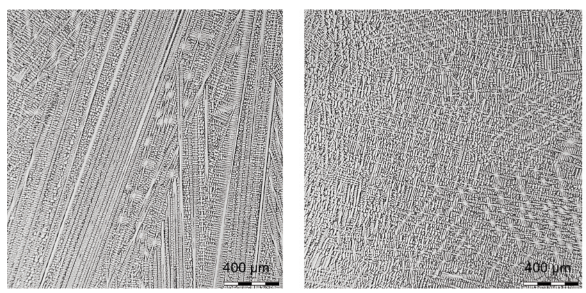


***Figure 3.*** *LM picture of the primary microstructure of Co-20Ni-9Al-7W-3Re-2Ti alloy*

The primarily revealed microstructure was typical for fast and directionally solidifying processes with heat dissipation effect, usually observed for casting into cold graphite molds. Detailed morphology of primary microstructure is visible in Fig. 4 and 5.

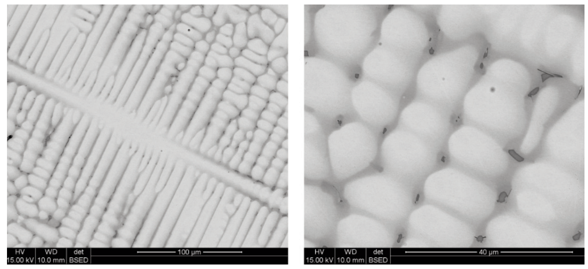

***Figure 4.*** *SEM picture of the primary microstructure of Co-20Ni-9Al-7W-3Re-2Ti alloy with visible precipitates in the interdendritic zones*

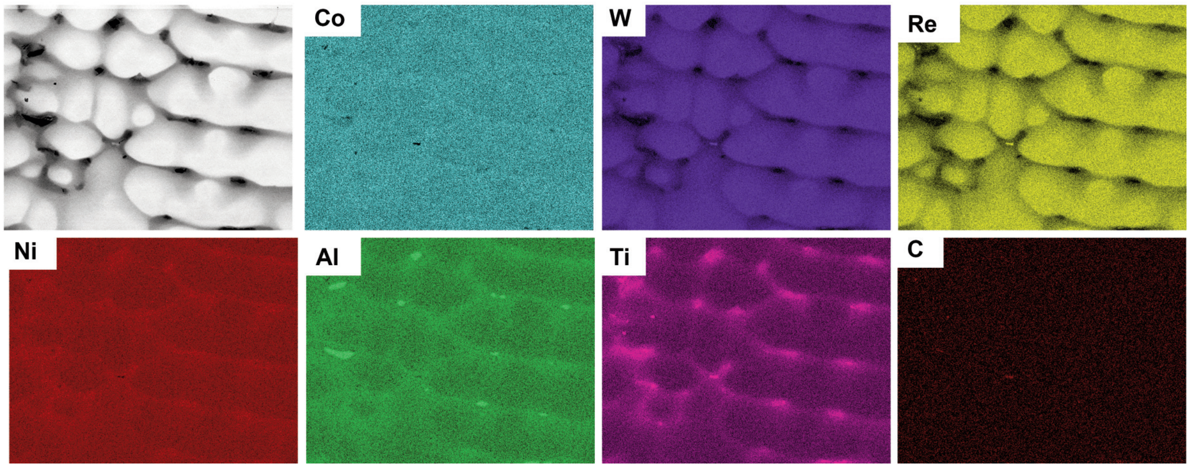


***Figure 5.*** *Alloying element maps of Co-20Ni-9Al-7W-3Re-2Ti alloy with a visible chemical constituent of precipitates in the interdendritic zones*

Special attention was taken to characterize the interdendritic area, as the zones important from the point of view of chemical composition homogenization during heat treatment processes.

The SEM analysis identified the small precipitates in interdendritic zones with a relatively high density of presences. Generally, those precipitates could be classified as W, Ti, and Re containing carbides and Al-Ti intermetallic phases. Those observations were confirmed by the EDS analysis in micro-areas presented in Fig. 6 and 7 (in the form of line distribution of alloying elements and point analysis, respectively), where zones rich in W and Ti were found (the EDS analysis also revealed C presence, but this method was not adequate to carbon analysis). Additionally, the areas affluent to Al and Ti were found as well. It suggested the presence of carbides of W and Ti (eventually Re) and Ti-Al compounds.

More precisely, the phase constituent of precipitates in micro-areas was described by the EBSD method. Results of those investigations were shown in Fig 8. These investigations confirmed that the interdendritic zones were rich in carbides precipitates of (W, Ti) $C_2$ type and intermetallic

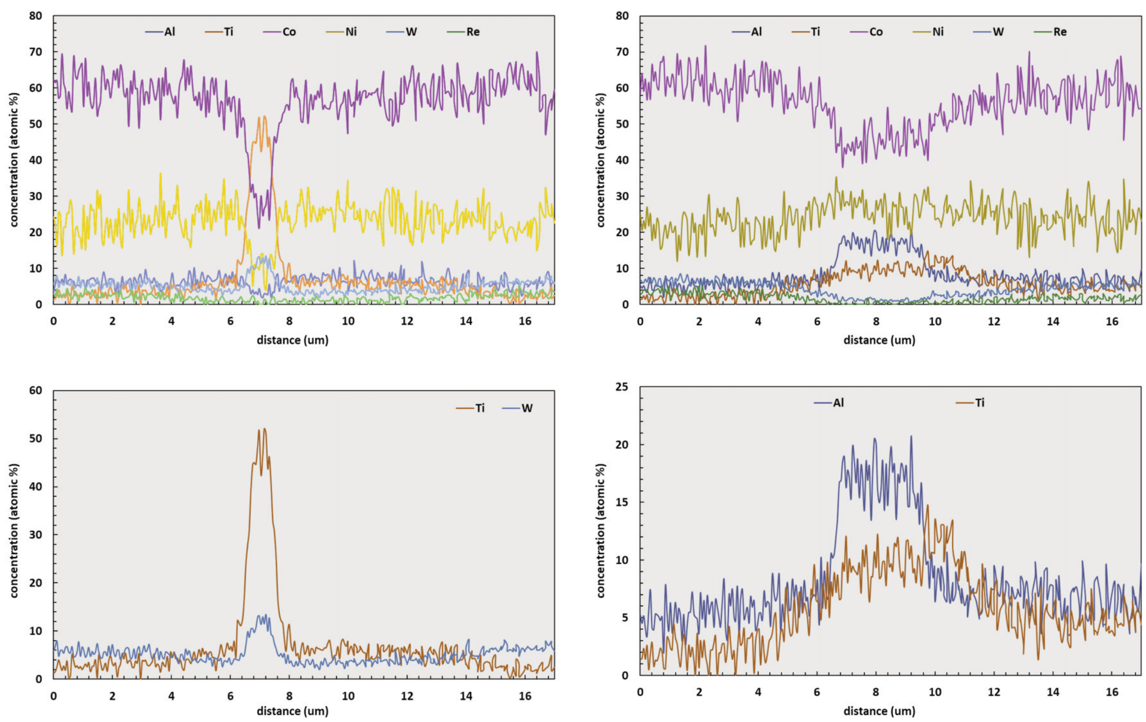


***Figure 6.*** *Chemical composition in micro-areas of Co-20Ni-9Al-7W-3Re-2Ti alloy – EDS line analysis*

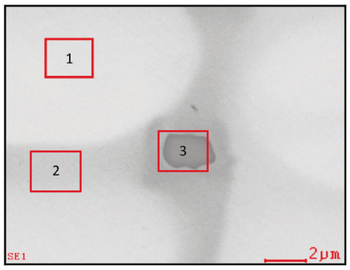

| Point 1 | Wt % | At % | Point 2 | Wt % | At % |
|---|---|---|---|---|---|
| Al | 02.34 | 06.61 | Al | 04.26 | 09.76 |
| W | 28.69 | 11.90 | W | 13.80 | 04.63 |
| Re | 09.16 | 03.75 | Re | 02.47 | 00.82 |
| Ti | 01.00 | 01.59 | Ti | 06.12 | 07.89 |
| Co | 44.72 | 57.85 | Co | 50.99 | 53.40 |
| Ni | 14.09 | 18.30 | Ni | 22.36 | 23.50 |

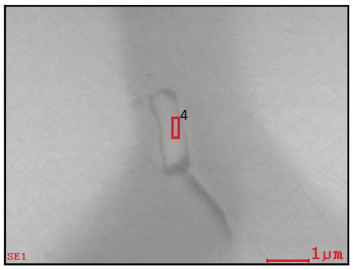

| Point 3 | Wt % | At % | Point 4 | Wt % | At % |
|---|---|---|---|---|---|
| Al | 10.15 | 20.22 | C | 12.99 | 48.70 |
| W | 06.23 | 01.82 | Al | 00.56 | 00.93 |
| Re | 00.89 | 00.26 | W | 41.82 | 10.25 |
| Ti | 10.31 | 11.57 | Ti | 32.92 | 30.96 |
| Co | 48.57 | 44.30 | Co | 08.32 | 06.55 |
| Ni | 23.85 | 21.83 | Ni | 03.41 | 02.61 |

***Figure 7.*** *Chemical composition in micro-areas of Co-20Ni-9Al-7W-3Re-2Ti alloy – EDS point analysis – average value from 10 random points*

compounds such as TiAl, $TiAl_2$, and $TiAl_3$. The Ti-Al compounds generally had beneficial effect on high temperature properties of materials [40]. It should be assumed that interdendritic zones were characterized by a strongly lower concentration of tungsten and rhenium than the in dendritic zone (assumption for solid solution). The same situation was detected in the case of cobalt, but the segregation effect was slightly lower. The contrary situation was observed for titanium distribution, where its concentration was ca. 3 times higher in the interdendritic zone (in at. %). In the case of Al, it was only ca. 0,5-time higher concentration. Ni concentration was only slightly higher. The effect of W, Al, and Co segregation was practically not observed for as-cast Co-9Al-9W alloy [41]. A similar tendency to segregation of W, Al, and Ni was observed in the case of Co-20Ni-7Al-7W alloy, but the scale of this effect was much lower [42].

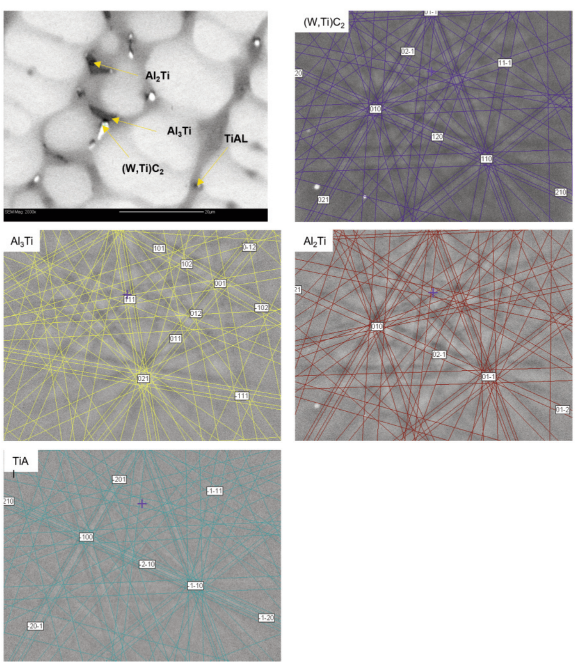


***Figure 8.*** *Phase's composition in micro-areas of Co-20Ni-9Al-7W-3Re-2Ti alloy – EBSD point analysis*

## 4. Conclusions

The presented analysis revealed that multi-component alloy of Co-20Ni-9Al-7W-3Re-2Ti type obtained by vacuum induction casting process was characterized by the high level of homogeneity of chemical composition. The observed differences of alloying element concentration in dendrites core and interdendritic zone were detectable but generally negligible. The strongest tendency to interdendritic segregation was observed for titanium and much lower for nickel and aluminium. The main problem related to the segregation effect was the formation of W and Ti-rich carbides and intermetallic compounds from the Ti-Al system.

### Authors contribution

*A. Tomaszewska – Funding acquisition, Conceptualization, Data caution, Methodology, Investigation, Writing – original draft, Writing – review & editing, Formal analysis, Validation, Visualization, Project administration.*

### Declaration of competing interest

*The author declare that she has no known* *competing financial interests or personal relationships that could have appeared to influence the work reported in this paper.*

**Acknowledgements**

T*his work was supported by the National Science Centre, Poland under grant number 2018/02/X/ST8/01817 (Miniatura II).*

**References**

[1] R.C. Reed, The Superalloys Fundamentals and Applications, Cambridge University Press, 2006.

[2] D. Coutsouradis, A. Davin, M. Lamberigts, Cobalt-based superalloys for applications in gas turbines, Materials Science and Engineering A, 88 (1987) 11-19. https://doi.org/10.1016/0025-5416(87)90061-9.

[3] D.L. Douglass, V.S. Bhide, E. Vineberg, The corrosion of some superalloys in contact with coal chars in coal gasifier atmospheres, Oxidation of Metals, 16 (1981) 29-79. https://doi.org/10.1007/BF00603744.

[4] N. Eliaz, G. Shemesh, R.M. Latanision, Hot corrosion in gas turbine components, Engineering Failure Analysis, 9 (2002) 31-43. https://doi.org/10.1016/S1350-6307(00)00035-2.

[5] S.-G. Kang and T. Kobayashi, Mechanical property of single phase Co-Ni-Cr-Mo based superalloy produced by cold working and recrystallization heat treatment, Materials Science Forum, 449-452 (2004) 573-576. https://doi.org/10.4028/www.scientific.net/MSF.449-452.573.

[6] W.H. Jiang, X.D. Yao, H.R. Guan, Z.Q. Hu, Secondary M6C precipitation in cobalt-base superalloy, Journal of Materials Science Letters, 8 (1999) 303–305.

[7] W.H. Jiang, X.D. Yao, H.R. Guan, Z.Q. Hu, Carbide behavior during high-temperature low cycle fatigue in cobalt-base superalloy, Journal of Materials Science, 4 (1999) 2859-2864. https://doi.org/10.1023/A:1004683301816

[8] P. Zieba, Microanalytical study of the discontinuous precipitation reaction in a Co–13 at. % Al alloy, Acta Materialia, 46 (1998) 369–377. https://doi.org/10.1016/S1359-6454(97)00200-0.

[9] T. Omori, Y. Sutou, K. Oikawa, R. Kainuma, K. Ishida, Shape memory effect in the ferromagnetic Co–14 at. % Al alloy, Scripta Materialia 52 (2005) 565–569. https://doi.org/10.1016/j.scriptamat.2004.12.001.

[10] T. Omori, Y. Sutou, K. Oikawa, R. Kainuma, K. Ishida, Shape memory and magnetic properties of Co–Al ferromagnetic shape memory alloys, Materials Science and Engineering A, 438 (2006) 1045–1049. https://doi.org/10.1016/j.msea.2005.12.068.

[11] H. Okamoto, Co-W (Cobalt-Tungsten), Journal of Phase Equilibria and Diffusion, 29 (2008), 119. https://doi.org/10.1007/s11669-007-9229-0.

[12] H. Okamoto, Co-Mo (Cobalt-Molybdenum), Journal of Phase Equilibria and Diffusion, 28 (2007) 300. https://doi.org/10.1007/s11669-007-9055-4.

[13] K.P. Gupta, The Co-Nb-W (Cobalt-Niobium-Tungsten) system, Journal of Phase Equilibria, 24 (2003) 82-85. https://doi.org/10.1007/s11669-003-0018-0.

[14] K.P. Gupta, The Co-Mo-Ta (Cobalt-Molybdenum-Tantalum) system, Journal of Phase Equilibria, 24 (2003) 186-189. https://doi.org/10.1361/105497103770330875.

[15] J. Sato, T. Omori, K. Oikawa, I. Ohnuma, R. Kainuma, K. Ishida, Cobalt-base high-temperature alloys, Science, 312 (2006) 90-91. https://doi.org/10.1126/science.1121738.

[16] C.S. Lee, Precipitation-hardening characteristics of ternary cobalt– aluminum–X alloys, University of Arizona, 1971.

[17] M. Korchynsky, R.W. Fountain, Precipitation phenomena in cobalt–tantalum alloys, Transactions of the Metallurgical Society of AIME, 215 (1959) 1033-1043.

[18] S.K. Makineni, B. Nithin, K. Chattopadhyay, A new tungsten-free γ-γ′ Co-Al-Mo-Nb-based superalloy, Scripta Materialia, 98 (2015) 36-39. https://doi.org/10.1016/j.scriptamat.2014.11.009.

[19] V.V. Kokorin, K.V. Chuistov, Initial stages of decomposition of supersaturated solid solutions Co–Ta and Co–Nb, Fiz Metallov Metalloved, 21 (1966) 311–314.

[20] R.D. Dragsdorf, W.D. Foreing, The intermetallic phases in the cobalt–tantalum system, Acta Crystallographica 15 (1962) 531–536.

[21] J. Dutkiewicz, G. Kostorz, Structure of martensite in Co–W alloys, Materials Science Engineering A, 132 (1991) 267–272. https://doi.org/10.1016/0921-5093(91)90383-X.

[22] S.K. Makineni, A. Samanta, T. Rojhirunsakool, T. Alam, B. Nithin, A.K. Singh, R. Banerjee, K. Chattopadhyay, A new class of high strength high temperature cobalt based γ-γ′ Co-Mo-Al alloys stabilized with Ta addition, Acta Materialia, 97 (2015) 29-40. https://doi.org/10.1016/j.actamat.2015.06.034.

[23] S.K. Makineni, B. Nithin, K. Chattopadhyay, Synthesis of a new tungsten-free γ-γ′ cobalt-based superalloy by tuning alloying additions, Acta Materialia, 85 (2015) 85-94. https://doi.org/10.1016/j.actamat.2014.11.016.

[24] Q. Yao, S.-L. Shang, Y.-J. Hu, Y. Wang, Y. Wang, Y.-H. Zhu, Z.-K. Liu, First-principles investigation of phase stability, elastic and thermodynamic properties in L12 Co3(Al,Mo,Nb) phase, Intermetallics, 78 (2016) 1-7. https://doi.org/10.1016/j.intermet.2016.08.002.

[25] T.M. Pollock, J. Dibbern, M. Tsunekane, J. Zhu, A. Suzuki, New Co-based gamma-gamma prime high-temperature alloys, JOM, 62 (2010) 58-63. https://doi.org/10.1007/s11837-010-0013-y.

[26] L. Klein, A. Bauer, S. Neumeier, M. Göken, S. Virtanen, High temperature oxidation of γ/γ′ - strengthened Co-based superalloys, Corrosion Science, 53 (2011) 2027-2034. https://doi.org/10.1016/j.corsci.2011.02.033.

[27] H.-Y. Yan, V.A. Vorontsov, D. Dye, Effect of alloying on the oxidation behavior of Co-Al-W superalloys, Corrosion Science, 83 (2014) 382-395. https://doi.org/10.1016/j.corsci.2014.03.002.

[28] M. Ooshima, K. Tanaka, N.L. Okamoto, K. Kishida, H. Inui, Effects of quaternary alloying elements on the γ′ solvus temperature of Co–Al–W based alloys with

fcc/L12 two-phase microstructures, Journal of Alloys and Compounds, 508 (2010) 71–78. https://doi.org/10.1016/j.jallcom.2010.08.050.

[29] L. Wang, M. Oehring, U. Lorenz, J. Yang, F. Pyczak, Influence of alloying additions on L12 decomposition in γ-γ′ Co-9Al-9W-2X quaternary alloys, Scripta Materialia, 154 (2018) 176–181. https://doi.org/10.1016/j.jallcom.2010.08.050.

[30] K. Shinagawa, T. Omori, K. Oikawa, R. Kainuma, K. Ishida, Ductility enhancement by boron addition in Co–Al–W high-temperature alloys, Scripta Materlialia, 61 (2009) 612–615. https://doi.org/10.1016/j.scriptamat.2009.05.037.

[31] Y.T. Xu, T.D. Xia, W.J. Zhao, X.J. Wang, Alloying element Nb effect on microstructure of Co–Al–W superalloy by vacuum arc melting, Applied Mechanics and Materials, 229 (2012) 63–67. https://doi.org/10.4028/www.scientific.net/AMM.229-231.63.

[32] F. Xue, H.J. Zhou, X.F. Ding, M.L. Wang, Q. Feng, Improved high temperature γ′ stability of Co–Al–W-base alloys containing Ti and Ta, Materials Letters, 112 (2013) 215–218. https://doi.org/10.1016/j.matlet.2013.09.023.

[33] L. Zhang, X. Qu, M. Qin, Rafi-ud-din, X. He, Ye Liu, Microstructure and mechanical properties of γ′ strengthened Co–Ni–Al–W-base ODS alloys, Materials Chemistry and Physics, 136 (2012) 371–378. https://doi.org/10.1016/j.matchemphys.2012.06.055.

[34] M. Titus, A. Suzuki, T.M. Pollock, Creep and directional coarsening in single crystals of new γ–γ′ cobalt-base alloys, Scripta Materialia, 66 (2012) 574-77. https://doi.org/10.1016/j.scriptamat.2012.01.008.

[35] K. Tanaka, M. Ooshima, N. Tsuno, A. Sato, H. Inui, Creep deformation of single crystals of new Co–Al–W-based alloys with fcc/L12 two-phase microstructures, Philosophical Magazine, 92 (2012) 4011-4027. https://doi.org/10.1080/14786435.2012.700416.

[36] M.S. Titus, Y.M. Eggeler, A. Suzuki, T.M. Pollock, Creep-induced planar defects in L12-containing Co- and CoNi-base single-crystal superalloys, Acta Materialia, 82 (2015) 530-539. https://doi.org/10.1016/j.actamat.2014.08.033.

[37] H.Y. Yan, V.A. Vorontsov, J. Coakley, N.G. Jones, H.J. Stone, D. Dye, Quaternary alloying effects and the prospects for a new generation of Co-base superalloys, in Superalloys 2002, E.S.Huron, R.C. Reed, M.C. Hardy, M.J. Mills, R.E. Montero, P.D. Portella, J. Telesman, eds. (The Minerals, Metals & Materials Society, Warrendale, PA, 2012); 705-714. https://doi.org/10.7449/2012/Superalloys_2012_705_714.

[38] L. Klein, M.S. Killian, S. Virtanen, The effect of nickel and silicon addition on some oxidation properties of novel Co-based high temperature alloys, Corrosion Science, 69 (2013) 43-49. https://doi.org/10.1016/j.corsci.2012.09.046.

[39] M. Knop, P. Mulvey, F. Ismail, A. Radecka, K.M. Rahman, T.C. Lindley, B.A. Shollock, M.C. Hardy, M.P. Moody, T.L. Martin, P.A.J. Bagot, D. Dye, A new polycrystalline Co-Ni superalloy, JOM, 66 (2014) 2495–2501. https://doi.org/10.1007/s11837-014-1175-9.

[40] D.-B. Wei, X. Zhou, F.-K. Li, M.-F. Li, S.-Q. Li, P.-Z. Zhang, Effects of Plasma Surface Ta Alloying on the Tribology Behavior of γ-TiAl, Journal of Mining and Metallurgy. Section B-Metallurgy, 57 (2021) 97-104. https://doi.org/10.2298/JMMB200617002W.

[41] T. Mikuszewski, A. Tomaszewska, G. Moskal, D. Migas, D. Niemiec, Characterization of primary microstructure of γ-γ' Co-Al-W cobalt-based superalloy, Materials Engineering, 5 (2017) 217-223. https://doi.org/10.15199/28.2017.5.3.

[42] A. Tomaszewska, G. Moskal, T. Mikuszewski, A. Płachta, G. Junak, Primary microstructure characterization of as-casted Co-20Ni-7Al-7W superalloy, Archives of Foundry, 19 (2019) 78-83. https://doi.org/10.24425/afe.2019.127143.

# KARAKTERIZACIJA PRIMARNE MIKROSTRUKTURE SUPERLEGURE Co-20Ni-9Al-7W-3Re-2Ti

**A. Tomaszewska**

Šleski tehnološki univerzitet, Fakultet za tehnologije materijala, Katovice, Poljska
Šleski tehnološki univerzite, Laboratorija za dizajn i proizvodnju materijala, Katovice, Poljska

***Apstrakt***

*U radu je prikazana karakterizacija primarne mikrostrukture nove superlegure na bazi Co tipa Co-20Ni-9Al-7W-3Re-2Ti. Ispitana legura je proizvedena inducijskim postupkom topljenja od čiste sirovine. Osnovni tehnološki problem vezan za postupak livenja višekomponentnih Co-Al-W-X legura je jaka podložnost interdendritskoj segragaciji legirajućih elemenata, posebno volframa i renijuma. Rezultati analize su pokazali da je uočeni efekat segragacije legirajućih elemenata bio detektovan i mnogo jači nego kod Co-9Al-9W i Co-20Ni-7Al-7W legura i odnosio se na migraciju titanijuma, nikla i aluminijuma u interdendritske prostore. Shodno tome, gradijent koncentracije volframa između dendritskih i interdendritskih zona je bio veći nego za Co-9Al-9W i Co-20Ni-7Al-7W legure. Ista situacija je bila i u slučaju renijuma i kobalta, ali koncentracija Co u interdendritskoj zoni je bila nešto malo niža.*

***Ključne reči:*** *Co-Al-W legura; Nova superlegura na bazi Co; Primarna mikrostruktura; Interdendritska segragacija*